

ChemComm

Accepted Manuscript



This is an *Accepted Manuscript*, which has been through the Royal Society of Chemistry peer review process and has been accepted for publication.

Accepted Manuscripts are published online shortly after acceptance, before technical editing, formatting and proof reading. Using this free service, authors can make their results available to the community, in citable form, before we publish the edited article. We will replace this *Accepted Manuscript* with the edited and formatted *Advance Article* as soon as it is available.

You can find more information about *Accepted Manuscripts* in the [Information for Authors](#).

Please note that technical editing may introduce minor changes to the text and/or graphics, which may alter content. The journal's standard [Terms & Conditions](#) and the [Ethical guidelines](#) still apply. In no event shall the Royal Society of Chemistry be held responsible for any errors or omissions in this *Accepted Manuscript* or any consequences arising from the use of any information it contains.



Journal Name

COMMUNICATION

Unexpected Functions of Oxygen in Chemical Vapor Deposition Atmosphere to Regulate Graphene Growth Modes

Received 00th January 20xx,
Accepted 00th January 20xx

Jing Li,^{a,b} Dong Wang*^a and Li-Jun Wan*^a

DOI: 10.1039/x0xx00000x

www.rsc.org/

Herein, by controlling the oxygen concentration in graphene growth process, we reveal that the ppm grade of oxygen in the graphene growth atmosphere can tune the graphene growth modes of multilayer growth and graphene etching fragments.

Due to the outstanding physical properties, such as ultrahigh carrier mobility,¹ thermal conductivity,² and uniform broadband photonic adsorption,³ graphene has attracted increasing interest for both fundamental science and technological applications.⁴ Currently, chemical vapor deposition (CVD) growth method on copper foils is one of the most promising synthetic approaches to obtain large-scale and high-quality graphene.⁵ In general CVD graphene growth process, carbon feed stocks (typically methane) dehydrogen on Cu substrate at high temperature in the presence of hydrogen, and results in the formation of active carbon species for graphene growth.^{6, 7} The role of hydrogen during such process is one of the most extensively researched topics, and currently it is widely accepted that the hydrogen plays a dual role of cocatalyst in the formation of active carbon species and etchant in the formation of stable graphene edge.⁸ Additionally, recent theoretical calculation of Ding et al. shows that the hydrogen atoms can attach onto the graphene edge and promote the growth of multi-layer graphene.⁹ However, the fact is that the concentration of hydrogen used in CVD process is different from lab to lab,^{8, 10, 11} and sometimes the as-obtained graphene shows obvious variation in thickness¹² and edge structure¹³ even with the same hydrogen partial pressure, suggests that the real role of H₂ is far from clear and/or some minority component may play important role in graphene synthesis.

Typically, people use 99.999% purity gases (the so-called ultrahigh purity gases) to avoid the effect of impurity.¹⁴

however, some recent reports demonstrate that the extremely minor amount of impurity in annealing gas¹⁵ and oxygen on Cu foil¹⁶ (lower than ppm grade) can influence the graphene etching structure and growth kinetics. To the best of our knowledge, no systemic work has been done to study the influence of such impurity on graphene structure during the CVD growth process. Thus it is easy to raise the skepticism whether there is some relationship between the various graphene growth structures and the ppm grade impurity, especially for oxygen.

Herein, the influence of oxygen concentration on graphene growth structure was systematically investigated by controlling the amount of oxygen in the CVD chamber during graphene growth process. Intriguingly, the phenomena such as multilayer graphene growth and graphene etching which have been ascribed to the effect of hydrogen can also be observed by simply adjusting the concentration of oxygen at ppm grade in the CVD atmosphere. In addition, the multilayer graphene staking structure is proven to be an inverted wedding-cake structure^{17, 18} that the multilayer graphene forms beneath the top graphene layer. The scanning electron microscopy (SEM) observation and X-ray photoelectron spectroscopy (XPS) characterization confirm that the penetration of oxygen into the space between graphene and Cu substrate accounts for multilayer graphene growth and etching effect. The demonstration of the dual role of minor amount of oxygen in multi-layer graphene growth and graphene etching effect will help deepen the understanding of CVD graphene growth mechanism and optimize the graphene growth process.

To clarify the influence of oxygen concentration on the graphene growth structure, a series of graphene were grown under varying concentration (from 0.8 to 200 ppm) of oxygen while at the same H₂ and CH₄ concentration. After growth and cooling down, the graphene were directly observed on Cu foil by SEM or transferred^{19, 20} onto 300 nm thick SiO₂/Si substrate and observed by optical microscope. As shown in far left column of Figure 1, in the growth atmosphere of ultrahigh purity Ar (oxygen ~ 0.8 ppm), graphene nuclei of monolayer form on Cu substrate after the growth time of 30 min, and further increasing the growth time to 180 min results in the

^a CAS Key Laboratory of Molecular Nanostructure and Nanotechnology and Beijing National Laboratory for Molecular Sciences, Institute of Chemistry, Chinese Academy of Sciences (CAS), Beijing 100190, P. R. China.

^b University of Chinese Academy of Sciences, Beijing 100049, P. R. China.

Electronic Supplementary Information (ESI) available: Experimental details, and the formation of multilayer and etching structure of graphene See DOI: 10.1039/x0xx00000x

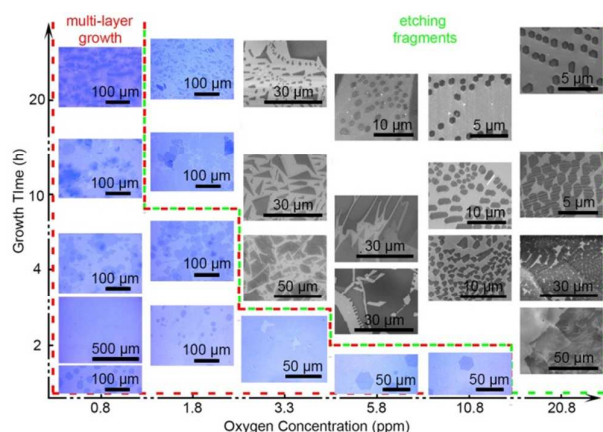


Fig 1. Dependence of graphene structures on the growth time and oxygen concentration in the growth atmosphere. The optical microscopy images are obtained on SiO₂/Si, and the SEM images are obtained on Cu foil.

full coverage of graphene film with the single layer ratio > 99% on Cu surface. Interestingly, different from the self-limiting growth mechanism,⁶ as further extending the growth time, multi-layer graphene comes into being even with the whole Cu surface covered by a completed graphene film. Increasing the growth time to 90 h can result in the formation of graphite-like film (as shown in Figure S1). After the introduction of extra oxygen, the growth of multilayer graphene tends to occur at the initial stage (short growth time), as shown in the zone marked by red dashed lines. The multilayer graphene formation process is demonstrated by a series of SEM images in Figure S2. Intriguingly, as further increasing growth time or oxygen concentration, the graphene finally develops into single layer fragments as shown in the zone marked by green dashed lines in Figure 1. In another word, the growth of multilayer graphene stops beyond certain growth time and then the continuous graphene film begin to break. Such observation can be ascribed to the etching effect of oxygen.²¹ The higher the oxygen concentration is, the earlier the graphene etching phenomenon tends to occur. For example, at the oxygen concentration of 20.8 ppm, the hexagonal graphene nuclei begin to break at the growth time of 120 min. When further increasing the oxygen concentration up to 40 ppm or even higher, no graphene but Cu₂O oxide layer can be observed on the Cu substrate (Figure S4-6), which should be contributed to the quenching effect of the oxygen overdose on active carbon species.

To identify the multi-layer graphene stacking structure, we use a PET/silicone film to tear the multi-layer graphene on SiO₂/Si substrate. As the interaction between the graphene and PET/silicone is weaker than that between graphene and SiO₂/Si substrate, but stronger than the interaction between interlayer graphene, tearing the multilayer graphene by PET/silicone film can tear the upmost-layer graphene.²² As shown by the yellow hollow arrow in Figure 2a-b, after tearing treatment, the top layer graphene was partially destroyed, while the second layer (as labeled by 2L) graphene edge keeps unchanged. This result reveals that the multilayer graphene has an inverted wedding-cake structure.¹⁷ Given that the upmost layer graphene film keeps continuous throughout the

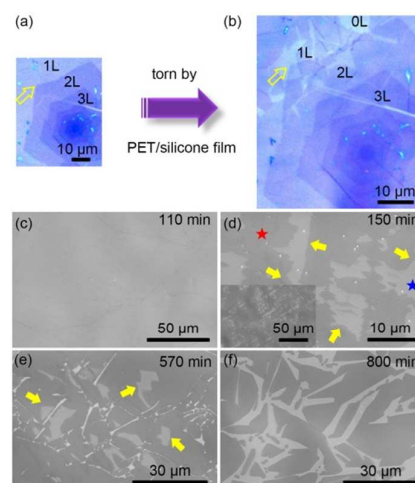


Fig 2. The multi-layer graphene stacking structure and oxygen penetration process. The in-situ optical microscopy images of multilayer graphene on SiO₂/Si substrate before (a) and after (b) the tearing treatment by PET/silicone film. (c-f) The SEM images show the typical evolution of polycrystalline graphene morphologies with growth time in the growth atmosphere containing 1.8 ppm O₂. The dark contrast zone as marked by red star in panel (d) is due to the oxygen intercalation between the graphene and the Cu substrate, and the insert is the large-scale SEM image. The bright contrast zone as marked by blue star correspondent to the initial graphene on Cu substrate. The yellow arrows in panel (e) mark the oxygen intercalation fronts.

multilayer graphene growth process and the low carbon solubility in Cu foil, (Figure S7-8) the active carbon species have to get into the space between graphene and Cu substrate by penetration from graphene grain boundaries or edges.^{9, 18} To further interpret the intercalation process, the graphene on Cu foil was characterized by SEM and XPS. As shown in Figure 2c-f, when extending growth time beyond the formation of the fully covered graphene on Cu foil, the brightness contrast changes can be observed begins from graphene wrinkle or graphene boundaries (Figure S10, as the yellow arrows show in Figure 2d) and extends progressively towards the center of graphene domains as time increasing. Similar contrast change has been observed for oxygen intercalates into the graphene and Ru substrate.²³ Additionally, the XPS is clearly indicative of cuprous oxides formation and oxygen intercalation. (Figure S9) Another interesting phenomenon is that, under higher oxygen concentration (5-25 ppm) in growth atmosphere, the etched graphene flakes can transform into parallel-edged hexagonal graphene fragment array structure. (as shown in the upper right panels of in Figure 1) Take the oxygen concentration of 10.8 ppm in the single-crystal graphene growth process for example, the hexagonal graphene fragments as shown in Figure 3a can be obtained after the growth time of 36 h, and the formation process of hexagonal graphene fragments can be seen in Figure S11. Given the high temperature and oxygen used during the etching process, the preservation of graphene quality becomes an important concern. Thus the hexagonal graphene fragment

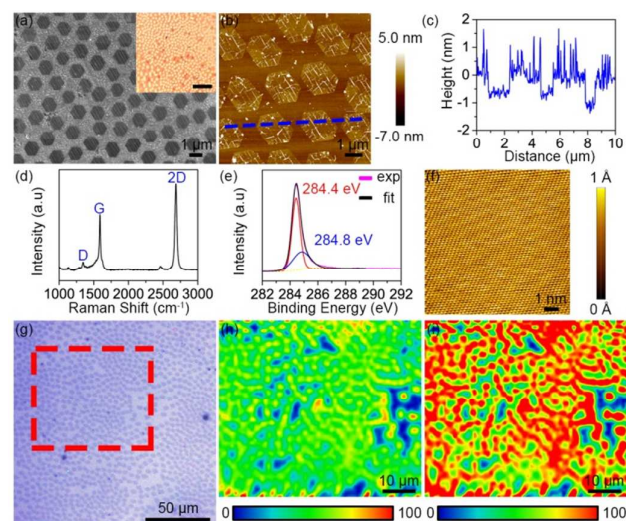


Fig 3. Characterization of etched hexagonal graphene fragment array. (a) Typical SEM and optical microscope (the insert figure) image of etched hexagonal graphene fragments on Cu surface. (b) The AFM morphology of the hexagonal graphene fragments transferred onto SiO₂/Si substrate. (c) The vertical height profile along the blue dashed line in the panel of (b). (d) The typical Raman spectra taken on the hexagonal graphene fragments on SiO₂/Si substrate. (e) XPS C1s spectra of the etched graphene fragments on Cu foil with the growth time of 60 h in the growth atmosphere containing 10.8 ppm oxygen. The magenta line represents the measured XPS spectrum, and the black line is the fitting curve. (f) The atomic structure of the etched graphene fragments which was observed by STM on Cu foil. (g) The optical microscopy of hexagonal graphene fragments of large scale on SiO₂/Si substrate. The G peak (h) and 2D (i) peak Raman mapping image of the graphene domains marked by the dotted box in panel (g).

array was further characterized by SEM, scanning probe microscopy and Raman spectroscopy. As graphene can protect the underlying Cu substrate from oxidation when heating in air atmosphere, the Cu surface where covered by graphene presents bright contrast after heating graphene/Cu foil in air at 200 °C for 2 min.²⁴ The optical image (upper insert of Figure 3a) of graphene/Cu presents bright spots pattern, which is consistent with the SEM result that the hexagonal structure is graphene rather than hexagonal graphene vacancy as observed previously.⁸ After transferred onto 300 nm SiO₂/Si substrate, the graphene structure was characterized by atomic force microscopy (AFM), and the vertical height profile (shown in Figure 3c) along the blue dashed line in Figure 3b demonstrates that the thickness of graphene fragments are about 1 nm, which is in accordance with the thickness of single-layer CVD graphene.^{11, 19} In addition, according to the Raman features (Figure 3d) of hexagonal graphene fragments structure [a symmetric 2D peak located ~2686 cm⁻¹ with the full width at half maximum of ~30 cm⁻¹, and the intensity ratio I_{2D}/I_G is higher than 2] further proves the graphene is of single-layer structure.²⁵ And the relatively low I_D (centered around 1347 cm⁻¹) intensity should be caused by the graphene edges

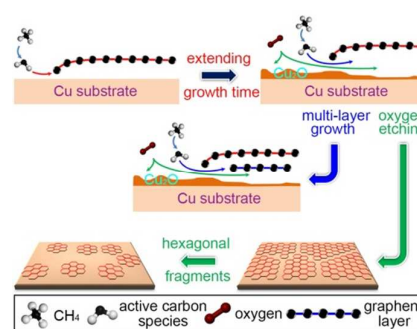


Fig 4. The proposed influence mechanism of oxygen on CVD graphene growth.

and transfer process. To further prove these hexagonal fragments structure is graphene rather than graphene oxide, the graphene fragments were characterized by XPS and scanning tunneling microscopy (STM). The dominant XPS (Figure 3e) spectrum component centered at 284.4 eV is correspondent to the sp² hybridization C-C bond, and the additional component appears at binding energies of 284.8 eV is assigned to the exchange interactions between the Cu valence electronic structure and the C1s core hole.²⁶ Besides, The graphene atomic structure as observed by STM shows holonomic and intact trigonal symmetry, which can further confirm that the hexagonal fragments are graphene rather than graphene oxide.²⁷ The Raman mapping results as presented in Figure 3f-g demonstrate the graphene fragments are of uniform thickness and structure.

On the basis of the results shown above, we propose that, (as shown in Figure 4) the oxygen in CVD chamber can intercalate into the space between the graphene and Cu substrate from the graphene edges and grain boundaries and form cuprous oxides beneath the graphene layer. This is supported by the SEM image of Figure 2c-f as well as the fact that the single crystal graphene starts to etch with higher oxygen concentration than that of polycrystalline graphene. The newly formed cuprous oxides can decouple the graphene^{23, 28} from the Cu substrate and thus increasing their distance. As a result, the intercalation of active carbon species and oxygen are further facilitated and serves as multilayer graphene growth feed stocks and graphene fragments etchant, respectively. We note the formation of graphene etching array structure is very different from the radial etching pits^{29, 30} as obtained by annealing treatment in oxygen atmosphere. This difference might be caused by the balanced effect of graphene etching of oxygen and regrowth caused by CH₄. However, the detailed explain of this intriguing phenomenon requires quantitative theoretical calculation, which will be pursued in further investigation.

In summary, the systematical investigation about the oxygen influence on graphene growth structure demonstrates that, minor amount of oxygen can obviously influence the multilayer growth and etching of graphene. This study reveals the role of minor amount of oxygen in multi-layer graphene growth and graphene etching effect, which will help promote the understanding of CVD graphene growth mechanism and

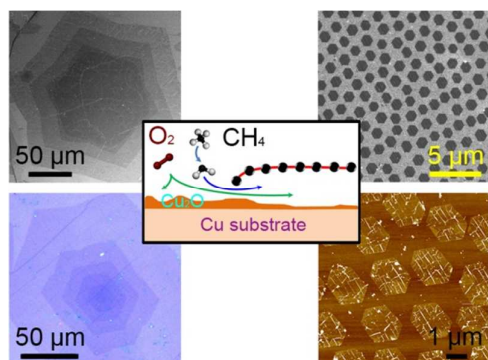
open up new perspective for multilayer graphene growth for device application.

This work was supported by the National Key Project on Basic Research (Grants2011CB808701, 2011CB932304), National Natural Science Foundation of China (21127901, 21233010, 21433011, 21373236), and the Strategic Priority Research Program of the Chinese Academy of Sciences (Grant No. XDB12020100).

30. L. Liu, S. Ryu, M. R. Tomasik, E. Stolyarova, N. Jung, M. S. Hybertsen, M. L. Steigerwald, L. E. Brus and G. W. Flynn, *Nano Letters*, 2008, **8**, 1965-1970.

Notes and references

1. K. S. Novoselov, A. K. Geim, S. V. Morozov, D. Jiang, Y. Zhang, S. V. Dubonos, I. V. Grigorieva and A. A. Firsov, *Science*, 2004, **306**, 666-669.
2. S. Chen, Q. Wu, C. Mishra, J. Kang, H. Zhang, K. Cho, W. Cai, A. A. Balandin and R. S. Ruoff, *Nat Mater*, 2012, **11**, 203-207.
3. R. R. Nair, P. Blake, A. N. Grigorenko, K. S. Novoselov, T. J. Booth, T. Stauber, N. M. R. Peres and A. K. Geim, *Science*, 2008, **320**, 1308.
4. K. S. Novoselov, V. I. Falko, L. Colombo, P. R. Gellert, M. G. Schwab and K. Kim, *Nature*, 2012, **490**, 192-200.
5. T. Kobayashi, M. Bando, N. Kimura, K. Shimizu, K. Kadono, N. Umezumi, K. Miyahara, S. Hayazaki, S. Nagai, Y. Mizuguchi, Y. Murakami and D. Hobaru, *Applied Physics Letters*, 2013, **102**, 023112.
6. X. Li, W. Cai, J. An, S. Kim, J. Nah, D. Yang, R. Piner, A. Velamakanni, I. Jung, E. Tutuc, S. K. Banerjee, L. Colombo and R. S. Ruoff, *Science*, 2009, **324**, 1312-1314.
7. C. Mattevi, H. Kim and M. Chhowalla, *Journal of Materials Chemistry*, 2011, **21**, 3324-3334.
8. I. Vlassiouk, M. Regmi, P. Fulvio, S. Dai, P. Datskos, G. Eres and S. Smirnov, *ACS Nano*, 2011, **5**, 6069-6076.
9. X. Zhang, L. Wang, J. Xin, B. I. Yakobson and F. Ding, *Journal of the American Chemical Society*, 2014, **136**, 3040-3047.
10. S. Bhaviripudi, X. Jia, M. S. Dresselhaus and J. Kong, *Nano Letters*, 2010, **10**, 4128-4133.
11. J. Bai, L. Liao, H. Zhou, R. Cheng, L. Liu, Y. Huang and X. Duan, *Nano Letters*, 2011, **11**, 2555-2559.
12. L. Liu, H. Zhou, R. Cheng, W. J. Yu, Y. Liu, Y. Chen, J. Shaw, X. Zhong, Y. Huang and X. Duan, *ACS Nano*, 2012, **6**, 8241-8249.
13. Z. Luo, S. Kim, N. Kawamoto, A. M. Rappe and A. T. C. Johnson, *ACS Nano*, 2011, **5**, 9154-9160.
14. Z. Yan, J. Lin, Z. Peng, Z. Sun, Y. Zhu, L. Li, C. Xiang, E. L. Samuel, C. Kittrell and J. M. Tour, *ACS Nano*, 2012, **6**, 9110-9117.
15. P. R. Kidambi, C. Ducati, B. Dlubak, D. Gardiner, R. S. Weatherup, M.-B. Martin, P. Seneor, H. Coles and S. Hofmann, *The Journal of Physical Chemistry C*, 2012, **116**, 22492-22501.
16. Y. Hao, M. S. Bharathi, L. Wang, Y. Liu, H. Chen, S. Nie, X. Wang, H. Chou, C. Tan, B. Fallahazad, H. Ramanarayan, C. W. Magnuson, E. Tutuc, B. I. Yakobson, K. F. McCarty, Y.-W. Zhang, P. Kim, J. Hone, L. Colombo and R. S. Ruoff, *Science*, 2013, **342**, 720-723.
17. N. Shu, W. Wei, X. Shirui, Y. Qingkai, B. Jiming, P. Shin-shem and F. M. Kevin, *New Journal of Physics*, 2012, **14**, 093028.
18. Q. Li, H. Chou, J.-H. Zhong, J.-Y. Liu, A. Dolocan, J. Zhang, Y. Zhou, R. S. Ruoff, S. Chen and W. Cai, *Nano Letters*, 2013, **13**, 486-490.
19. J. Li, H. Ji, X. Zhang, X. Wang, Z. Jin, D. Wang and L.-J. Wan, *Chemical Communications*, 2014, **50**, 11012-11015.
20. W. Z. HU BaoShan, AGO Hiroki, JIN Yan, XIA MeiRong, LUO ZhengTang, PAN QingJiang, LIU YunLing, *SCIENCE CHINA Chemistry*, 2014, **57**, 895-901.
21. G. Dobrik, L. Tapasztó and L. P. Biró, *Carbon*, 2013, **56**, 332-338.
22. X.-D. Chen, Z.-B. Liu, C.-Y. Zheng, F. Xing, X.-Q. Yan, Y. Chen and J.-G. Tian, *Carbon*, 2013, **56**, 271-278.
23. P. Sutter, J. T. Sadowski and E. A. Sutter, *Journal of the American Chemical Society*, 2010, **132**, 8175-8179.
24. C. Jia, J. Jiang, L. Gan and X. Guo, *Sci. Rep.*, 2012, **2**, 707.
25. A. C. Ferrari, J. C. Meyer, V. Scardaci, C. Casiraghi, M. Lazzeri, F. Mauri, S. Piscanec, D. Jiang, K. S. Novoselov, S. Roth and A. K. Geim, *Physical Review Letters*, 2006, **97**, 187401.
26. P. R. Kidambi, B. C. Bayer, R. Blume, Z.-J. Wang, C. Baetz, R. S. Weatherup, M.-G. Willinger, R. Schloegl and S. Hofmann, *Nano Letters*, 2013, **13**, 4769-4778.
27. X. Chen, S. Liu, L. Liu, X. Liu, X. Liu and L. Wang, *Applied Physics Letters*, 2012, **100**, 163106.
28. S. Gottardi, K. Müller, L. Bignardi, J. C. Moreno-López, T. A. Pham, O. Ivashenko, M. Yablonskikh, A. Barinov, J. Björk, P. Rudolf and M. Stöhr, *Nano Letters*, 2015, **15**, 917-922.
29. S. Choubak, M. Biron, P. L. Levesque, R. Martel and P. Desjardins, *The Journal of Physical Chemistry Letters*, 2013, **4**, 1100-1103.

Figure for Table of contents

The ppm grade of oxygen in CVD atmosphere can obviously tune the graphene growth modes of multilayer and etching fragments.